Impurity interactions in disordered metals. II. Conductance fluctuations in mesoscopic systems

M. T. Béal-Monod
Physique des Solides, Université de Paris–Sud, 91405 Orsay, France

G. Forgacs
Department of Physics, Clarkson University, Potsdam, New York 13376
(Received 21 March 1991)

We reexamine the theory of conductance fluctuations in mesoscopic systems, in particular, the sensitivity of such fluctuations to the motion of one single impurity. In contrast with all previous theories on the subject, we do not assume the impurities to be independent. Instead, we take into account the existence of a local atomic order between the impurities which results from their mutual interactions. We show that, to the lowest order in this local ordering, its overall effect cancels out from the sum of all contributing diagrams, so that the universal character of the conductance fluctuations is still preserved. In contrast, it does show up when a single impurity is moved, in which case the resulting conductance fluctuations become dependent on the degree of electronic disorder and dimensionality. It is conjectured that, as the amount of impurity local ordering increases, it will also modify the universal character of the conductance fluctuations.

I. INTRODUCTION

After the important progress made in the understanding of Anderson localization of macroscopic systems [recalled in the preceding paper (I)], the next hallmark has been the discovery of the "universal" conductance fluctuations in disordered electronic systems of "mesoscopic" sizes.[1–3] It turned out that conductance fluctuations in such systems are independent (between broad limits) of the degree of disorder, size, and dimensionality of the sample. Moreover, it has been shown[4,5] that, in thin films of mesoscopic size, the displacement of a single impurity induces conductance fluctuations as large as those produced by changing the entire sample. It was argued in Ref. 5 that this observation may have implications for the understanding of $1/f$ noise.

The theories of Refs. 1–5 assumed the electrons to be noninteracting and the impurities to be independent. We recently showed[6] that interactions between the impurities (inducing a local ordering between them), in addition to affecting the conductivity of the system (as discussed at length in I), also modifies the conductance fluctuations in "mesoscopic" samples. In Ref. 6, however, we confined ourselves to a study of the modifications arising in one of the "two-diffuson" diagrams considered in Refs. 1 and 2. We then found, from the computation of such a diagram, that the universal character of the conductance fluctuations is lost since the amplitude of the conductance fluctuations clearly depended on the degree of electronic disorder and dimensionality. Based on this result, we assumed, in Ref. 6, that our finding, concerning the loss of the universal nature of the conductance fluctuations, would remain valid also when the contribution of all other relevant diagrams is included.

In the present paper, we wish to complete our preliminary work of Ref. 6, using the basic ingredients described in the preceding paper (I). We include, here, the contributions of all the two-diffuson diagrams contributing to the conductance fluctuations of mesoscopic systems.[3] (Diagrams with two diffusons have indeed been shown[3] to be the only ones contributing to the conductance fluctuations.) We show, in Sec. II, that the qualitative conclusion of our preliminary work of Ref. 6 is drastically modified when the sum of all possible contributions is evaluated. This amounts to the cancellation of the overall impurity local ordering effect, although it shows up in each two-diffuson diagram individually. We thus recover the universal result of Refs. 1 and 2 for independent impurities. Such a cancellation is similar to the one found in I for the localization contribution $(\sigma_{MC}+\delta\sigma_{MC})$ to the conductivity. In Sec. III, we reexamine the sensitivity of conductance fluctuations in mesoscopic systems to the motion of a single impurity. There, we show that the conclusions of Refs. 4 and 5 must be revised: the local ordering between the impurities, resulting from their mutual interactions, does have an overall effect. As a consequence, the conductance fluctuations induced by the motion of a single impurity in a two-dimensional system do not produce the same fluctuations as those resulting from changing the entire sample as found in Ref. 5. In Sec. IV, we conclude our work by contrasting the results of Secs. II and III, and analyzing the effect of increasing the impurity local ordering. As in Paper I we give our results for $D=1$, 2, and 3.

II. CONDUCTANCE FLUCTUATIONS IN MESOSCOPIC SYSTEMS IN THE PRESENCE OF IMPURITY INTERACTIONS

In the present section, we recall the main steps to calculate the conductance fluctuations in mesoscopic systems, taking into account impurity interactions.[6]

According to the classical result, the variance of the dimensionless conductance Var $(g)=\langle g^2\rangle-\langle g\rangle^2$ behaves as

$$\mathrm{Var}(g)\sim\langle g\rangle^2/L^D\sim L^{D-4}\ , \tag{1}$$

where L is the characteristic linear size of the system. The breakthrough of Refs. 1–3 was to show that quantum-mechanical effects modify the above result so that

$$\mathrm{Var}(g)\sim L^{D-4}\int_{L^{-1}}(q^2)^{-2}d^Dq\ . \tag{2}$$

The additional integral in (2) corresponds to the two-diffuson diagram contribution arising in the calculation of the variance of the conductivity $\langle\sigma^2\rangle-\langle\sigma\rangle^2$, with $g=\sigma L^{D-2}$. $\mathbf{q}$ is the common momentum involved in both diffusons. We recall that a diffuson Γ_d is an infinite ladder of single impurity scattering lines in the particle-hole channel, which satisfies the Bethe-Salpeter equation shown in Fig. 1 of I. In what follows, Γ_d will be simply denoted by Γ. Equation (2) yields

$$\mathrm{Var}(G)\sim(e^2/h)^2,\quad G=(e^2/h)g\ . \tag{3}$$

In Ref. 3 it was shown that the diagrams contributing to Var (g) are the two-diffuson diagrams recalled here in Fig. 1, with their detailed structures displayed in Fig. 2. It can indeed be rigorously proved[3] that only *two*-diffuson diagrams contribute to the conductance fluctuations.

In Ref. 6, we reevaluated one of the two-diffuson diagrams [namely, the one in Fig. 1(a)], taking into account the interactions between impurities along the lines described in I. We found that the universal result (3) obtained in the absence of impurity interactions is modified by these interactions and depends explicitly on dimensionality and the degree of electronic disorder. Although we emphasized that other diagrams [in particular, those in Figs. 1(b)–1(e)] should also be considered, we assumed that our conclusion would not be qualitatively changed and that the impurity local ordering would still break the universal character of the conductance fluctuations.

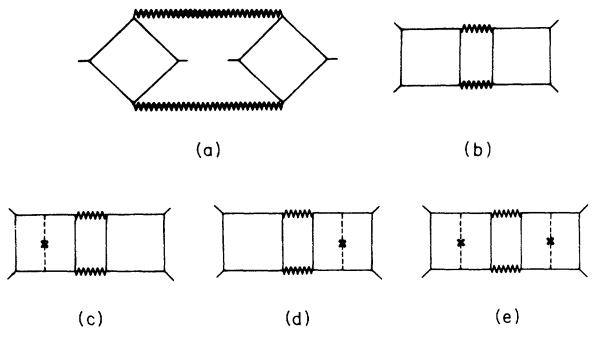

FIG. 1. The two-diffusion diagrams entering the calculation of the conductance fluctuations in the independent impurity model (Ref. 3). The wiggly lines denote the diffuson whereas the dotted line with a cross stands for a single impurity line. See Fig. 2 for details.

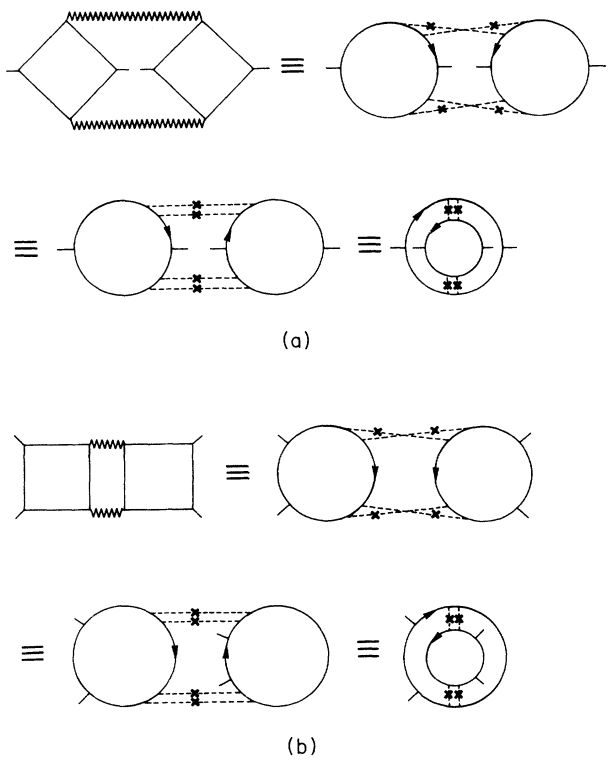

FIG. 2. The details of the Hikami-type boxes of Fig. 1. An ensemble of two dotted lines with crosses denote an infinite ladder diffuson Γ_d, as shown in Fig. 1 of I. Figures 1(c), 1(d), and 1(e) are obtained from (b) with the addition of single impurity lines.

First, we show that, in the presence of impurity interactions, there are more diagrams to consider than those displayed in Fig. 1. These additional diagrams are shown in Figs. 3 and 4. The diagrams in Figs. 1, 3, and 4 are the ones which contribute to first order in λ, where λ contains the impurity interaction strength [as defined in Eq. (3) of I]. Then we show that the effect of the impurity local ordering disappears from the sum of diagrams in Figs. 1, 3, and 4 when these are evaluated to first order in λ. As a consequence, the effect of impurity interaction shows up in the conductance fluctuations only through the upper cutoff in the integral in (2). This result is analogous to the one found in I for the localization contribution to the conductivity in the presence of impurity local ordering.

The algebra is quite straightforward and is done the way it was described in Ref. 6 for the diagram of Fig. 1(a). Each one of the two diffusons contributes through the quantity

$$\Gamma=\Gamma_0\{1+\lambda[M_1^2(x)-3M_0^2(x)]\}\ ,$$
$$\Gamma_0=\frac{1}{2\pi N(\varepsilon_F)\tau_0^2}\frac{\Theta(\Omega_1)\Theta(\Omega_2)}{D_0q^2+\Omega_1+\Omega_2}\ , \tag{4}$$

where Ω_1 and Ω_2 are the appropriate Matsubara frequencies of the electron lines on either side of the diffuson. $M_0(x)$ and $M_1(x)$ are given, respectively, by formulas (5) and (7) in I. $x=k_Fd$, k_F is the Fermi momentum and d

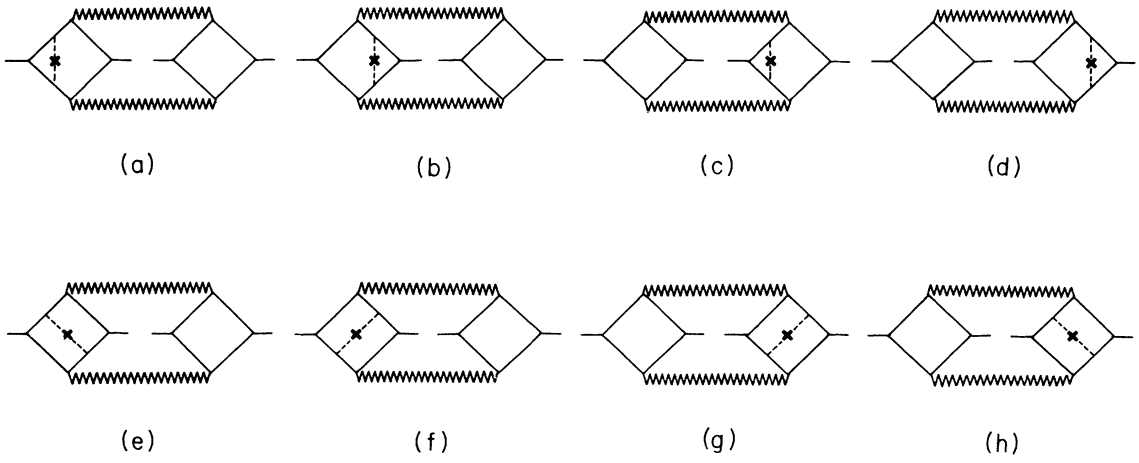

FIG. 3. Extra diagrams to be added to Fig. 1(a) in the presence of finite impurity interactions.

the nearest-neighbor distance of the lattice model used to represent our system of a binary alloy of host and impurity atoms. (For more details, see I and Ref. 5 in that paper.) The extra single impurity line (with a cross), involved in Figs. 1, 3, and 4, corresponds to the effective scattering potential modified by impurity interactions and is given by formulas (1) and (3) in I. With all the previously defined terms, we find the following results. As far as the λ dependence of Fig. 1(a) is concerned (the only one studied in Ref. 5), it contributes as

$$\begin{aligned}(\tau')^6\Gamma^2 &\simeq \tau_0^6[1+6\lambda M_0^2(x)] \\ &\quad\times\Gamma_0^2\{1+2\lambda[M_1^2(x)-3M_0^2(x)]\} \\ &= \tau_0^6\Gamma_0^2[1+2\lambda M_1^2(x)]\ ,\quad \lambda\ll 1\ .\end{aligned} \tag{5}$$

However, the extra diagrams in Fig. 3 amount to adding to the above expression the quantity

$$-\tau_0^6\Gamma_0^2[2\lambda M_1^2(x)]\ . \tag{6}$$

Therefore, adding the contributions of Figs. 1(a) and 3, the term $\lambda M_1^2(x)$ cancels out. One can easily check that the same kind of cancellation occurs between the diagrams of Figs. 1(b)–1(e) and those of Fig. 4. Finally, in three dimensions, the contributions of the diagrams in Figs. 1(a) and 3, denoted, respectively, by $K^{(1a)}$ and $K^{(3)}$ yield

$$K^{(1a)}+K^{(3)}=(16k_F^4/3)T^2\sum_{n,n'}\int\frac{d^3q}{(2\pi)^3}Y\ , \tag{7}$$

with

$$\begin{aligned}Y=&\frac{\Theta(\omega_{n+\nu})\Theta(-\omega_{n'})\Theta(\omega_n)\Theta(-\omega_{n'+\nu'})}{(\omega_{n+\nu}-\omega_{n'}+D_0q^2)(\omega_n-\omega_{n'+\nu'}+D_0q^2)} \\ &+\frac{\Theta(\omega_{n+\nu})\Theta(-\omega_{n'})\Theta(-\omega_n)\Theta(\omega_{n'+\nu'})}{(\omega_{n+\nu}-\omega_{n'}+D_0q^2)(\omega_{n'+\nu'}-\omega_n+D_0q^2)} \\ &+\frac{\Theta(-\omega_{n+\nu})\Theta(\omega_{n'})\Theta(-\omega_n)\Theta(\omega_{n'+\nu'})}{(\omega_{n'}-\omega_{n+\nu}+D_0q^2)(\omega_{n'+\nu'}-\omega_n+D_0q^2)}\ ,\end{aligned} \tag{8}$$

where $\omega_{n+\nu}$ and ω_n are the Matsubara frequencies in-

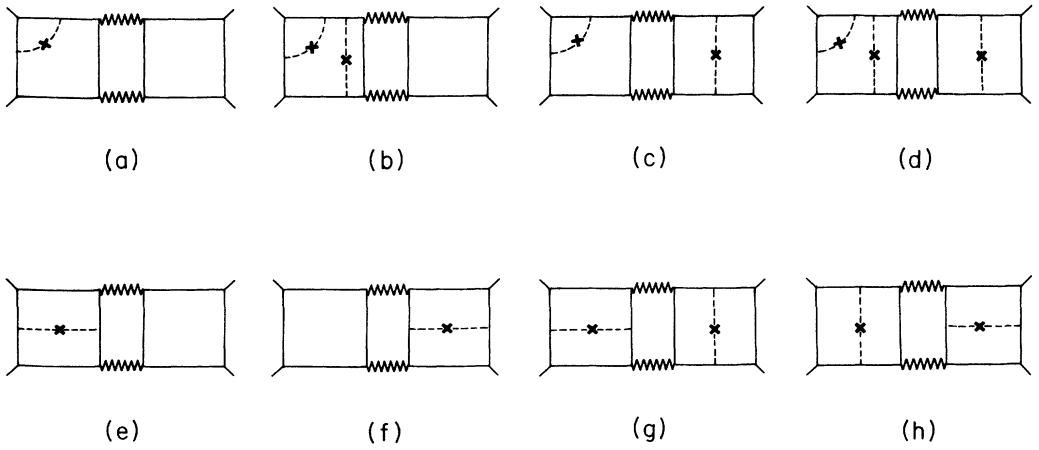

FIG. 4. Extra diagrams to be added to Figs. 1(b)–1(e), in the presence of finite impurity interactions. Twelve other diagrams analogous to (a)–(d) are not shown but do contribute as well; they are obtained by dressing each of the other three external vertex corners analogously to what is shown in (a)–(d).

volved in one of the loops, with ω_ν being the external incoming and outgoing frequency; $\omega_{n'+\nu'}$ and $\omega_{n'}$ are those of the other loop, with $\omega_{\nu'}$ the corresponding external frequency.

On the other hand, the contributions of Figs. 1(b)–1(e) and 4 give

$$K^{(1b)}+K^{(1c)}+K^{(1d)}+K^{(1e)}+K^{(4)}=4k_F^4T^2\sum_{n,n'}\int\frac{d^3q}{(2\pi)^3}Y . \tag{9}$$

[Note that there is only a numerical factor difference between (7) and (9).]

Compared to the above results (7) and (9), the full contribution of Fig. 1(a) alone (computed in Ref. 5) is

$$K^{(1a)}=(16k_F^4/3)[1+2\lambda M_1^2(x)]T^2\sum_{n,n'}\int\frac{d^3q}{(2\pi)^3}Y . \tag{10}$$

In Figs. 1, 3, and 4, each diagram, individually, contains a multiplicative factor, a signature of the impurity local ordering. However, when the sum of all the diagrams is performed, the impurity interaction effect *disappears,* at least to first order in λ. The impurity interaction effect survives only in the upper limit of the remaining integral over $\mathbf{q}$, since $q<(k_Fl')^{-1}$ [with l' being the mean free path in the presence of impurity local ordering, given by formula (4) in I], as was the case for the localization contribution to the conductivity in I. However, here, due to the convergence of the $\mathbf{q}$ integral at the upper limit, this cutoff is much less important than in the conductivity case ($\int d^D\mathbf{q}/q^4$ compared to $\int d^D\mathbf{q}/q^2$).

Therefore the universal character of the conductance fluctuations, emphasized in Refs. 1–3 for independent impurities, still survives here (to first order in λ), provided that the linear dimension L of the mesoscopic sample is larger than l',

$$\begin{aligned} &L\gg l' ,\\ &(l')^{-1}=l_0^{-1}[1-\lambda M_0^2(x)] . \end{aligned} \tag{11}$$

(l_0 is the mean free path in the absence of impurity interactions.) As discussed in I, there is no physical reason for such a cancellation to survive when the impurity local ordering gets stronger. In fact upon increasing the local ordering, the impurities eventually will develop long-range spatial order either in the form of long-range atomic order or segregation, depending on the sign of their interactions. This, in turn, reacts on the conductivity of macroscopic systems as well as on the conductance fluctuations of mesoscopic ones. Furthermore, even to first order in λ, there are diagrams which we have neglected both here and in I because they would give smaller contributions, involving higher powers of $(\varepsilon_F\tau_0)^{-1}$ (in the metallic regime $\varepsilon_F\tau_0\gg1$). Such contributions are impurity interaction dependent and there is no *a priori* reason why they would also cancel to all powers of $(\varepsilon_F\tau_0)^{-1}$. Calculations to higher orders in λ for fixed $(\varepsilon_F\tau_0)^{-1}$ values or to first order in λ but to higher powers of $(\varepsilon_F\tau_0)^{-1}$ are out of the scope of the present paper but should be kept in mind before concluding that the impurity local ordering plays no role at all.

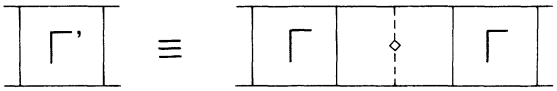

FIG. 5. The diffuson Γ' when one impurity is moved from its original position. The extra diamond-type impurity scattering line is given in the text by formula (12).

III. SENSITIVITY OF THE CONDUCTANCE FLUCTUATIONS TO THE MOTION OF A SINGLE IMPURITY IN THE PRESENCE OF IMPURITY INTERACTIONS

In order to evaluate the modifications of the conductance fluctuations upon moving a single impurity a distance $\delta\mathbf{r}$ away from its original position, we follow the recipe described in Ref. 5. In that paper, it was pointed out that moving a single impurity amounts to replacing one of the two diffusons in the conductance fluctuations diagrams, Γ, by Γ' as shown in Fig. 5. The extra vertex in Fig. 5 involves a new scattering potential different from the one in formula (1) of I, through the quantity Z' as follows:

$$|U'(\mathbf{p}'-\mathbf{p})|^2=Z'[1+\delta Z(|\mathbf{p}'-\mathbf{p}|)] , \tag{12a}$$

$$Z'=(Z/N_i)\mathrm{Re}(1-e^{i\delta\mathbf{r}\cdot(\mathbf{p}'-\mathbf{p})}) . \tag{12b}$$

N_i is the number of impurities and Z is given below formula (1) of I. For the derivation of (12b), see the Appendix. [In the work of Ref. 5, impurity interactions were absent, corresponding to $\delta Z=0$ in (12a).] Here the analytic expression corresponding to Fig. 5 is given by

$$\Gamma'=\Gamma^2ZN_i^{-1}\left[(B')^2-A'(\delta\mathbf{r})A'(-\delta\mathbf{r})+\frac{\lambda}{2z}[-2A'(\mathbf{d})A'(-\mathbf{d})+A'(\mathbf{d}+\delta\mathbf{r})A'(-\mathbf{d}-\delta\mathbf{r})+A'(\mathbf{d}-\delta\mathbf{r})A'(-\mathbf{d}+\delta\mathbf{r})]\right] . \tag{13}$$

z is the number of nearest neighbors in the model lattice describing the binary alloy of host and impurity atoms. B' and A' have been defined in Ref. 6. A tedious but straightforward calculation shows that B' and $A'(\mathbf{s})A'(-\mathbf{s})$, needed in (13), reduce to

$$\begin{aligned} &(B')^2=Z^{-2}[1+2M_0^2(x)] ,\\ &A'(\mathbf{s})A'(-\mathbf{s})=(B')^2M_0^2(k_Fs) \end{aligned} \tag{14}$$

(we recall that $x=k_Fd$). Here $s=|\mathbf{s}|$ denotes the modulus of the argument appropriate to each one of the

various A' functions appearing in (13), equal to $\pm\delta r, \pm d, \pm|\mathbf{d}+\delta\mathbf{r}|, \pm|\mathbf{d}-\delta\mathbf{r}|$. $M_0(k_F s)$ is given by formula (5) of I, but with $k_F s$ replacing x. One finally gets

$$\Gamma' = \Gamma^2 \Lambda ,$$

$$\Lambda = Z^{-1} N_i^{-1} (1 - M_0^2(y) + \lambda \{ M_0^2(x)[1 - 2M_0^2(xy)] + R(x,y) \})$$

$$= \Lambda(\lambda = 0) + \lambda \, \delta\Lambda , \tag{15}$$

with $y = k_F \, \delta r$ and

$$R(x,y) = \frac{1}{2z} \sum_{\mathbf{d}} [M_0^2(k_F|\mathbf{d}+\delta\mathbf{r}|) + M_0^2(k_F|\mathbf{d}-\delta\mathbf{r}|)] \tag{16}$$

we obtain the following partial results.

In three dimensions (3D), R reduces to

$$R_{3D} = \frac{1}{4xy} \left[\ln \left| \frac{x+y}{x-y} \right| + \mathrm{Ci}(2|x-y|) - \mathrm{Ci}(2(x+y)) \right] , \tag{17}$$

where Ci is the integral cosine of the argument.[7]

In 2D, R can be represented by an integral which is well behaved and can be evaluated numerically, namely,

$$R_{2D} = \frac{1}{\pi} \int_{Y_-}^{Y_+} \frac{J_0^2(k_F \sqrt{Y})}{\sqrt{Y_+ - Y} \sqrt{Y - Y_-}} dY \tag{18}$$

with $Y_{+,-} = (d \pm \delta r)^2$; J_0 is the Bessel function of the first kind and index 0.[8]

In 1D, R reads

$$R_{1D} = \cos^2 x \cos^2 y + \sin^2 x \sin^2 y \tag{19}$$

so that Γ' takes a very simple form,

$$\Gamma'_{1D} = (\Gamma^2)_{1D} Z^{-1} N_i^{-1} \sin^2(k_F \, \delta r)(1+\lambda) .$$

Now, let

$$\delta K = K_b - K_a , \tag{20}$$

where K_b, K_a are the values of the sum of the diagrams in Figs. 1, 3, and 4, respectively, before and after moving one impurity a distance $\delta\mathbf{r}$ away from its original position; obviously K_b involves diagrams with two identical diffusons Γ, while, in K_a, one of the two diffusons has been replaced by Γ'. We will compute δK in the presence of impurity local ordering and compare it with the result of Ref. 5, δK_{FLS}, obtained in the absence of impurity interactions

$$\delta K_{\mathrm{FLS}} = C \alpha(k_F \, \delta r) ,$$
$$C = (e^2/h)^2 L^D (N_i l_0^D)^{-1} (L/l_0)^{2-D} . \tag{21}$$

$\alpha(k_F \, \delta r)$ in (21), resulting from an angular average, depends on dimensionality[5]

$$\alpha(k_F \, \delta r) = 1 - M_0^2(k_F \, \delta r) , \tag{22}$$

where M_0 was given in formula (5) of I, with x replaced here by $(k_F \, \delta r)$, with different forms depending on D [for convenience, we recall that $M_0(x) = \sin(x)/x$ in 3D, $J_0(x)$ in 2D, $\cos x$ in 1D]. The contribution of Fig. 1(a) to K_a defined above, amounts to changing the two-diffuson diagram into a three-diffuson one, by replacing one of the Γ in Fig. 1(a) by Γ' depicted in Fig. 5. This leads, in the final $\mathbf{q}$ integral [like the one in (2)], to a $(1/q^2)^3$ dependence instead of the $(1/q^2)^2$ dependence in the absence of impurity interactions.

Now, we have to, not only consider Fig. 1(a), but we must also collect the contributions of all the diagrams of Figs. 1, 3, and 4, where we move one impurity a distance $\delta\mathbf{r}$ away. This is done in two ways: either as in the case of Ref. 5 by moving one impurity in one of the two diffusons as in Fig. 5, thus yielding three-diffuson diagrams, with an ultimate $(1/q^2)^3$ divergence, as noted above, or by moving that impurity which corresponds to a single impurity line (the dotted line with a cross in Figs. 1, 3, and 4). In such a case, the corresponding diagrams will still contain only two diffusons and will thus involve only $(1/q^2)^2$ divergences, the two diffusons being unaffected by the motion of the extra impurity.

Clearly, moving one impurity in one of the two diffusons will yield the dominant contribution [due to the resulting $(1/q^2)^3$ singularity] and we retain only these in the following. Compared with the discussion in the preceding section, instead of $(\tau')^6 \Gamma^2$ in (5), we have now to deal with the modified quantity

$$(\tau')^6 \Gamma^2 \rightarrow 2(\tau')^6 \Gamma \Gamma' . \tag{23}$$

The factor 2 here is due to the fact that Γ' can replace either one of the two diffusons Γ. Γ' is given by (15). Therefore, each one of the two series $(K^{(1a)} + K^{(3)})$ and $(K^{(1b)} + K^{(1c)} + K^{(1a)} + K^{(1e)} + K^{(4)})$ involves

$$2\{(\tau')^6 \Gamma\Gamma' - [(\tau')^6 \Gamma\Gamma']_{\lambda=0}[2\lambda M_1^2(x)]\} = 2\tau_0^6 \Gamma_0^3 (\{1 + 3\lambda[M_1^2(x) - M_0^2(x)]\}[\Lambda(\lambda=0) + \lambda\delta\Lambda] - 2\lambda M_1^2(x)\Lambda(\lambda=0)) \tag{24}$$

$$= \tau_0^6 \Gamma_0^3 \frac{1}{Z} \frac{1}{N_i} ([1 - M_0^2(y)]\{1 + \lambda[M_1^2(x) - M_0^2(x)]\} + \lambda[-M_0^2(x) + R(x,y)]) . \tag{25}$$

In addition to (24) and (25), the two series of diagrams contain, similarly to (7) and (9), the numerical coefficients $(\frac{16}{3})$ and 4. Therefore, compared to δK_{FLS} [which involved only the diagram of Fig. 1(a), with one diffuson Γ replaced by Γ' of Fig. 5, and $\lambda = 0$], we have

$$\frac{\delta K}{\delta K_{\rm FLS}}=\frac{2(\frac{16}{3}+4)}{\frac{16}{3}[1-M_0^2(y)]}([1-M_0^2(y)]+\lambda\{[1-M_0^2(y)][M_1^2(x)-M_0^2(x)]-M_0^2(x)+R(x,y)\}) \tag{26}$$

With C given in (21) and $\alpha(y)=\alpha(k_F\,\delta r)$ of (22), we get

$$\delta K=\tfrac{7}{2}C(\alpha(k_F\,\delta r)+\lambda\{\alpha(k_R\,\delta r)[M_1^2(k_Fd)-M_0^2(k_Fd)]-M_0^2(k_Fd)+R(k_Fd,k_F\,\delta r)\})\ . \tag{27}$$

One checks that, for $\delta r=0$, δK vanishes as it should. Note that, in 1D, δK takes the simple form

$$(\delta K)_{\rm 1D}=\tfrac{7}{2}C\sin^2(k_F\,\delta r)[1-2\lambda\cos(2k_Fd)] \tag{28}$$

with the interesting consequences that, for $\lambda=\frac{1}{2}$,

$$(\delta K)_{\rm 1D}\propto\sin^2(k_F\,\delta r)\sin^2(k_Fd)\ ,$$

and when $\lambda=-\frac{1}{2}$,

$$(\delta K)_{\rm 1D}\propto\sin^2(k_F\,\delta r)\cos^2(k_Fd)\ .$$

In either cases, $(\delta K)_{\rm 1D}$ oscillates, separately, with (k_Fd) and $(k_F\,\delta r)$ and vanishes for certain values of these arguments.

In 2D and 3D, as $\delta r\to\infty$, while $\delta K_{\rm FLS}\to C$, we find here that

$$(\delta K)_{\rm 2D,3D}\to C\{1+\lambda[M_1^2(k_Fd)-2M_0^2(k_Fd)]\}\qquad\text{as } \delta r\to\infty\ . \tag{29}$$

Therefore, in contrast to the results of the previous section, where the impurity interaction effects canceled out (to first order in λ), here they give a nonvanishing contribution when one impurity is moved away. As a consequence, in particular in 2D, moving a single impurity does *not* induce the same conductance fluctuations as those resulting from the changing of the entire sample, as found in Ref. 5. The fluctuations which are induced depend on dimensionality and the degree of electronic disorder. Such modifications should be kept in mind when extending the theory to high temperatures to explore $(1/f)$-noise phenomena, as suggested in Ref. 5.

IV. DISCUSSION

In this work similarly to I, we only compute the effect of impurity interactions to first order in λ, i.e., to the lowest order in the impurity local ordering. In that sense, we can understand that the impurity interactions disappear in the results of Sec. II (except for the upper cutoff in q), while they play a role in Sec. III. Indeed when only a small amount of impurity local ordering is involved, the overall conductance fluctuations may remain unaffected. In contrast, when one moves a single impurity a distance $\delta\mathbf{r}$ away, one probes a local effect and, there, even a tiny amount of impurity local ordering will be significant.

We expect, on physical grounds—although we cannot prove it mathematically at this point— higher-order contributions in λ (i.e., a larger amount of local ordering between the impurities), to show up in the localization contribution to the conductivity of I as well as in the conductance fluctuations of Sec. II of the present paper. In this case, using the terminology of the renormalization group (see I for details), interactions between the impurities should lead to the change of the conductance fixed point, as compared to the independent impurity case. This, in turn, would show up in the breakdown of the universal character of the conductance fluctuations. Our results, valid to first order in λ, allow us only to demonstrate the tendency towards the breakdown of this universal character. Evaluating the integral in (2), one has

$$\mathrm{Var}(g)\sim(4-D)^{-1}[1-(l_0/L)^{4-D}]\ , \tag{30}$$

where, for $L\gg l_0$, the second term is negligible and one gets the universal result of the independent impurity model. In the presence of impurity interactions, l_0 in (30) is replaced by l', and (30) now becomes

$$\mathrm{Var}(g)\sim(4-D)^{-1}[1-(l'/L)^{4-D}]\ . \tag{31}$$

According to (11), for $\lambda>0$, $l'>l_0$. Therefore the second term within the square brackets in (31) increases, upon increasing λ, and may become comparable to the first term, while the corresponding term in (30) remains small compared to the first one.

ACKNOWLEDGMENTS

The authors are indebted to S. Feng for several valuable discussions on the topic. They also benefited from useful comments by R. Harris and B. Al'tshuler. The financial support of NATO Grants No. 0736/88 and No. CRG8800736 is gratefully acknowledged. Laboratoire de Physique des Solides is a Laboratoire associé au Centre National de la Recherche Scientifique.

APPENDIX

In this appendix, we show that displacing a single impurity by $\delta\mathbf{r}$ is equivalent to introducing a modified scattering potential given by (12). The diagrams in Figs. 1, 3, and 4, involve, each one of them, two bubbles which correspond to conductivities with different impurity configurations. In particular, for the electron-impurity interaction in one of the bubbles, one takes

$$U(\mathbf{r})=U_0\sum_{i=1}^{N_i}\delta(\mathbf{r}-\mathbf{R}_i)\ . \tag{A1}$$

Here $\mathbf{R}_i$ and U_0 stand, respectively, for the position vector and the strength of the scattering potential in the absence of interactions between the impurities. In the other bubble

$$\bar{U}(\bar{r})=U_0\sum_{i\,(\neq j)}\delta(\bar{\mathbf{r}}-\mathbf{R}_i)+U_0\delta(\bar{\mathbf{r}}-\mathbf{R}_j-\delta\mathbf{r})\ . \tag{A2}$$

Here $\delta\mathbf{r}$ is a fixed vector, whereas $\mathbf{R}_k$ are independent random variables which can take any value within the volume of the system, with probability L^{-D}. In calculating the diagrams in Figs. 1, 3, and 4, one needs $\langle U(\mathbf{r})U(\bar{\mathbf{r}})\rangle - \langle U(\mathbf{r})\bar{U}(\bar{\mathbf{r}})\rangle$, where $\langle\ \rangle$ denotes the average with respect to the probability distribution of the $\mathbf{R}$ (this means integration with respect to the $\mathbf{R}_k$ with the constant weight L^{-D} for each value of $k=1,2,\ldots,N_i$). Since

$$\langle U(\mathbf{r})U(\bar{\mathbf{r}})\rangle = Z[\delta(\mathbf{r}-\bar{\mathbf{r}})+(N_i-1)/2] \tag{A3}$$

by choosing appropriately the zero of the potential, the constant term in (A3) can be discarded. Performing an analogous calculation for $\langle U(\mathbf{r})\bar{U}(\bar{\mathbf{r}})\rangle$, upon Fourier transformation, we obtain

$$|U(\mathbf{k})^2| = \frac{1}{N_i}\mathrm{Re}\int d^D(\mathbf{r}-\bar{\mathbf{r}})e^{i\mathbf{k}\cdot(\mathbf{r}-\bar{\mathbf{r}})} \times[\langle U(\mathbf{r})U(\bar{\mathbf{r}})\rangle - \langle U(\mathbf{r})\bar{U}(\bar{\mathbf{r}})\rangle] = \frac{U_0^2}{N_i}[N_i-(N_i-1+\mathrm{Re}e^{i\mathbf{k}\cdot\delta\mathbf{r}})]\ . \tag{A4}$$

This result is equivalent to expression (12b) given in the text with $\mathbf{k}\equiv(\mathbf{p}'-\mathbf{p})$. This derivation also shows that the extra vertex [yielding (12b)] should *not* affect the individual Green's functions involved in the bubbles of Figs. 1, 3, and 4; it acts only *between* the bubbles (as shown in Fig. 5), contrary to what was assumed in Ref. 9.

[1]B. L. Al'tshuler, Pis'ma Zh. Eksp. Teor. Fiz. **41**, 530 (1985) [JETP Lett. **41**, 648 (1985)]; B. L. Al'tshuler and D. E. Khmel'nitskii, *ibid.*, **42**, 291 (1985) [*ibid.* **42**, 359 (1985)]; A. D. Stone, Phys. Rev. Lett. **54**, 2692 (1985); P. A. Lee and A. D. Stone, *ibid.*, **55**, 1622 (1985); Y. Imry, Europhys. Lett. **1**, 249 (1986).

[2]P. A. Lee *et al.*, Phys. Rev. B **35**, 1039 (1986).

[3]B. L. Al'tshuler and b. I. Shklovskii, Pis'ma Zh. Eksp. Teor. Fiz. **91**, 220 (1986) [JETP **64**, 127 (1986)]. It is pointed out in this work that some diagrams were missing in Ref. 2.

[4]B. L. Al'tshuler and B. Z. Spivak, Pis'ma Zh. Eksp. Teor. Fiz. **42**, 363 (1985) [JETP Lett. **42**, 447 (1985)].

[5]S. Feng *et al.*, Phys. Rev. Lett. **56**, 1960 (1986); **56**, 2772(E) (1986). There is a small error in this work: in the expression (4) for the function $\alpha(k_F\delta r)$, the factor $\frac{1}{2}$ should be replaced by 1 everywhere. In addition, the form given there for $\alpha(k_F\delta r)$ is valid only in 3D, as we explain in the present paper, before and after formula (22).

[6]M. T. Béal-Monod and G. Forgacs, J. Phys. (Paris) **50**, 2709 (1989). Note that in formula (16) of that paper the factor (e^2/h) should be raised to the second power: $(e^2/h)^2$.

[7]See, for instance, E. Jahnke and F. Emde, *Tables of Functions with Formulas and Curves* (Dover, New York, 1943).

[8]See, for instance, I. S. Gradshteyn and I. W. Ryzhik, *Tables of Integrals, Series and Products* (Academic, New York, 1965).

[9]S. Hershfield, Phys. Rev. B **37**, 8557 (1988).